

Data-Free Class Incremental Gesture Recognition via Synthetic Feature Sampling

Zhenyu Lu
Carnegie Mellon University
zhenyulu@andrew.cmu.edu

Hao Tang
Carnegie Mellon University
hao.tang@vision.ee.ethz.ch

Abstract

*Data-Free Class Incremental Learning (DFCIL) aims to enable models to continuously learn new classes while retaining knowledge of old classes, even when the training data for old classes is unavailable. Although explored primarily with image datasets by researchers, this study focuses on investigating DFCIL for skeleton-based gesture classification due to its significant real-world implications, particularly considering the growing prevalence of VR/AR headsets where gestures serve as the primary means of control and interaction. In this work, we made an intriguing observation: skeleton models trained with base classes (even very limited) demonstrate strong generalization capabilities to unseen classes without requiring additional training. Building on this insight, we developed **Synthetic Feature Replay (SFR)** that can sample synthetic features from class prototypes to replay for old classes and augment for new classes (under a few-shot setting). Our proposed method showcases significant advancements over the state-of-the-art, achieving up to 15% enhancements in mean accuracy across all steps and largely mitigating the accuracy imbalance between base classes and new classes.*

1. Introduction

Class incremental learning (CIL) refers to the learning paradigm wherein models are continuously updated as new class data is introduced. This area has gained significant attention as researchers recognize that data in real-world scenarios typically arrives incrementally rather than all at once. Although considerable progress has been made in class incremental learning [8, 25, 34, 41, 51], most of the research has focused on experimenting with images as the primary modality. However, the recent emergence of large pre-trained, visual or visual-language models, such as CLIP [33], DINO [4], SAM [19] and their variations, has demonstrated remarkable generalizability, showcasing impressive zero-shot performance. This development, to some extent, challenges the significance of class incremental learn-

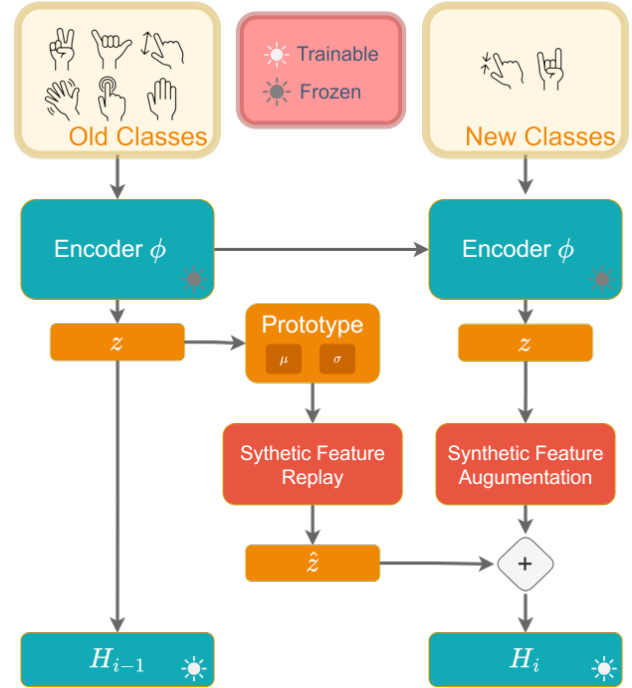


Figure 1. Overall Pipeline. (1) Compute and save class prototypes from the embedding space. (2) Sample synthetic old class features from the saved class prototype using Algo. 1. (3) **Only in the few shot setting**, sample synthetic new class feature using Algo. 2 to augment the new class data. (4) Combine new and old class features together to train the classifier.

ing research focused solely on images. We wouldn't be too surprised if leveraging large pre-trained vision models could surpass state-of-the-art performance on common image datasets that most class incremental learning studies tested on, either in zero-shot set or given a few shot prompts.

Therefore, we argue that class incremental learning research should address specific real-world problems or be differentiated by modalities, as different modalities may exhibit distinct interclass properties as the CIL algorithm primarily experimented on image datasets might not be a universal solution adaptable to other modalities. Unlike the

abundance of image sources readily available from the Internet, human-related data sources are more limited due to factors such as labor costs and privacy concerns associated with collecting data from individuals. These types of data sources may align better with the continuous availability of data. With the increasing trend in Virtual Reality (VR) technology and the growing market penetration of high-quality VR devices like Oculus Quest and Vision Pro, personal VR/AR devices are becoming more prevalent.

Gesture-based interaction is the primary means of controlling AR/VR headsets [15, 16]. Class incremental learning for skeleton-based gesture recognition shows promising value; for example, users may register and customize their own gestures for various functions. However, data privacy and security are significant concerns for human-related computer vision tasks, as even skeletal gestures can inadvertently reveal personal identity information. Thus, restricting the setting to be data-free, meaning that only data used to train newly introduced classes is available without access to training data for old classes, becomes especially important and natural.

In this study, we explore Data Free Class Incremental Learning (DFCIL) for Skeleton Gesture, a new research domain introduced by BOAT-MI [1]. Unlike BOAT-MI which involves data synthesis via model inversion and retraining of the whole model. We decide to keep the feature extractor consistently frozen, as we observe that the model trained for skeletal data exhibits a much greater ability to generalize to new classes than images without additional updating. Then, by modeling class feature space as a multivariate normal distribution characterized by a prototype defined by its mean and covariance, we can sample synthetic features that can be used for both old class replay and new class augmentation.

In summary, the key contributions of this paper are as follows:

- We reveal that models trained for skeleton gestures inherently possess better generalization ability for unseen classes without requiring additional training.
- Based on this observation, we proposed a novel **Synthetic Feature Replay (SFR)** algorithm that circumvents the need for challenging synthetic data generation, which is typically used in existing DFCIL methods. Our approach is not only faster and simpler, but also significantly outperforms current SOTA methods across all tested datasets.
- Additionally, we examined the effect of shot size within the Few Shot Class Incremental Learning (FSCIL) context and found that sampling synthetic features for new classes combined with a carefully designed filtering mechanism can alleviate performance degradation caused by limited data availability.

2. Related Work

Data Free Class Incremental Learning. Regularization-based approaches [20, 25, 51] are a major category to address catastrophic forgetting of old classes [28] present in DFCIL. Knowledge distillation is a quite useful technique that is usually used in conjunction with other approaches. [5, 17, 24, 25, 34, 46, 47] use knowledge distillation to ensure that the model is updated without deviating too much from its frozen copy of its previous state. Model expansion [42, 43, 48] is another effective technique, allowing the model to dynamically grow as needed. Replay-based methods for DFCIL usually involve generating pseudo-samples of previously seen classes to mitigate the forgetting of old class knowledge. Training a sample generator during the pretraining stage is an effective way [8, 37], but model inversion is a technique that can invert the model to obtain fake old class samples without training an additional generator [13, 38, 52].

Few-Shot Class Incremental Learning. FSCIL [41] is a setup that imposes additional restrictions on the sample size of incremental classes beyond those in DFCIL. One strategy widely used in few-shot class incremental learning is to keep the backbone encoder frozen and update only the classifier to adapt to new classes. These methods focus either on creating better pre-trained base models [40, 56, 57], or designing novel classifiers [53]. Constructing a class prototype [3, 14, 21, 27], originally proposed by ProtoNet [39], primarily used for a few-shot learning, has also proved useful in creating the classifier for FSCIL as well [45, 58]. Our approach also adopts such a frozen encoder strategy, but instead of directly using class prototypes to build the classifier, we sample synthetic features from class prototypes and train the classifier along with the sampled features.

DFCIL for Skeleton-Based Gesture Recognition. Using skeletal data, instead of raw image frames, for gesture recognition, shows great value for its reduced data complexity and therefore effective processing and privacy protection. Deep learning approaches such as CNN-LSTM [31], GCNs [7, 23, 49], transformers [6, 36, 44, 55], typically show superior performance for skeleton-based gesture recognition. ST-GCN [49] is a popular GCN-based model that can automatically learn both spatial and temporal patterns. DGSTA [6] is a transformer-based model that applies multi-head attention to spatial and temporal edges, respectively, for hand gesture recognition.

Class incremental learning for skeleton data, especially in the data-free setting, is still a valuable but underexplored domain. To the best of our knowledge, BOAT-MI [1] represents pioneering work in investigating data-free class incremental learning of gestures by developing a model

inversion-based approach to generate synthetic samples and replay them during training new classes. Therefore, we follow their setup to run our experiments and benchmark against them.

3. Preliminaries

3.1. Problem Definition

Data free class-incremental learning is the setup such that a model need to continue learning novel classes while not forgetting knowledge about old classes. Firstly, the entire dataset is divided into \mathcal{N} subsets $\mathcal{D}_i = \{(X, Y) : Y \in \mathcal{C}_i, i \in T\}$. Here, i denotes the i -th incremental session and \mathcal{C}_i denotes the label space, noting that the class space introduced are exclusive between different steps. The base model is trained with \mathcal{D}_0 and the model needs to update based on the information from $\{\mathcal{D}_1, \mathcal{D}_2, \dots, \mathcal{D}_{\mathcal{N}-1}\}$ continuously, with data from previous incremental sessions no longer available. However, the test set for the i -th incremental session should encompass all classes seen before, such that $\mathcal{C}_i^{test} = \cup_{j=0}^i \mathcal{C}_j$.

In addition to DFCIL, few-shot class-incremental learning (FSCIL) imposes a even stricter constraint where the sample size for each class during the incremental session is limited. Each task can be represented as an N -way K -shot classification task, where N classes are learned in the current step, with K samples available for each class.

3.2. Metric Learning

Metric learning or frozen encoder-based approaches are usually composed of two parts: a feature encoder ϕ and a classifier \mathcal{H} . Given the input and label of sample (x, y) , the feature of x can be denoted as $z = \phi(x)$ and the predicted label can be obtained by $\hat{y} = \mathcal{H}(z)$.

The encoder ϕ pre-trained at the base stage is kept frozen for all upcoming incremental steps while only the classifier \mathcal{H}_i for each step updates continuously.

3.3. Instantaneous Forgetting Measure (IFM)

The central dilemma in class incremental learning revolves around balancing the preservation of knowledge from old tasks with the ongoing learning of new tasks. However, many existing studies [8, 26, 53, 57] tend to over-prioritize overall accuracy as the primary evaluation metric, often overlooking the imbalance between the accuracy of the base classes and the incremental classes. For instance, training directly on new classes without any form of regularization can lead the model to quickly forget old knowledge, causing the new class accuracy to significantly outperform the old classes. On the contrary, frozen encoder-based image CIL approaches tend to perform much poorer on newly introduced classes compared to base classes that are inherently trained for the base model.

Instantaneous Forgetting Measure [2] is an important metric evaluating such imbalances:

$$IFM = \frac{|L - G|}{L + G} \times 100\%, \quad (1)$$

where L represents the local accuracy solely over the novel classes introduced during a continual learning step, while G signifies the global accuracy over all classes encountered by the model up to that stage, including the novel classes. IFM is expressed as a percentage, with 0% indicating perfect balance ($G = L$) and 100% indicating pure imbalance (either $G = 0$ or $L = 0$).

4. What to Replay? Embeddings or Samples

Synthetic replay-based DFCIL approaches [1, 8, 13, 37, 52] typically involve training an additional generator or using model inversion to create fake data. However, generating such samples poses significant challenges, as pre-training a generator during the previous step can be cumbersome, and the quality of samples generated through model inversion may suffer, especially for skeletal gesture movements that entail both spatial and temporal changes. BOAT-MI [1] proposed a novel boundary-aware sampling mechanism from class prototypes to generate the best synthetic samples via model inversion, but they still have trouble generating high-quality samples.

Thus, is there a way to bypass the challenging data synthesis step? Our proposed approach directly utilizes synthetic features sampled from prototypes to replay the old class and facilitate the training of the new class, when the samples of the newly class are limited, as illustrated in Figure 1. The effectiveness of our approach is rooted in a key observation.

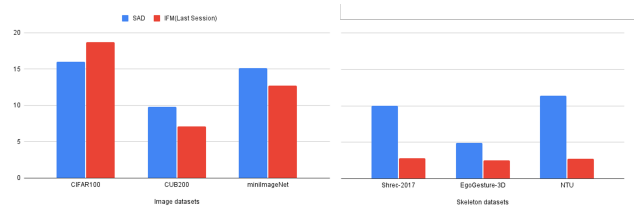
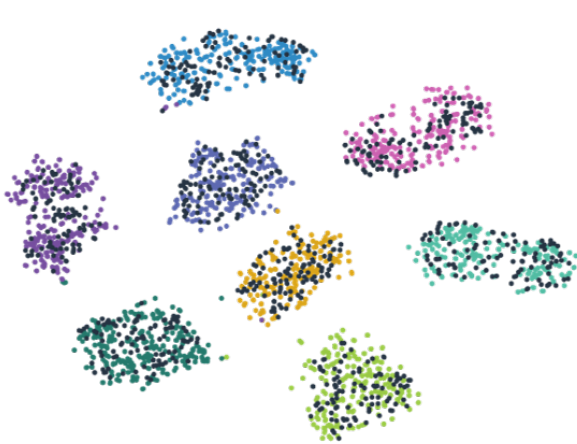


Figure 2. A overall comparison between DFCIL on image datasets (Left) and skeleton datasets (Right), shows the performance on skeleton datasets generally superior to that on image datasets (We use our proposed approach to generate experiment result for skeleton datasets and use TEEN [45] (SOTA) for image datasets). Session Accuracy Delta (SAD) measures the gap between the accuracy of the base session and the accuracy of the final session after the model has processed all data. IFM (last session) measures the Instantaneous Forgetting Measure of the last session.

Skeleton models trained on base classes can generalize to unseen classes well. Frozen encoder-based approaches



(a) T-SNE visualization comparing ground truth features and sampled synthetic features. The sampled features are colored in black.



(b) T-SNE visualization comparing features of old and new classes. The features of the newly introduced classes are circled in red.

Figure 3. A toy experiment on Shrec-2017, three new hand gesture classes were added to a model pre-trained on eight base classes. A similar experiment was conducted on an image dataset for comparison, and the details can be found in the appendix.

are widely used in FSCIL. However, when applied to image domains, they often suffer from severe accuracy imbalance, and the model struggles on new classes, as illustrated in Figure 2, which explains why this strategy is not commonly used for DFCIL when the sample size is abundant. As noted in TEEN [45], new classes tend to be classified into the most similar base classes. Despite their attempts to address this issue through calibration, the accuracy gap between base classes (70%-80%) and new classes (40%-50%) remains substantial. This discrepancy leads to an Incremental Forgetting Measure (IFM) score of approximately 20%, indicating the model’s difficulty in adapting to unseen classes.

However, we found that using a frozen encoder is particularly well suited for skeleton modality, as our experiments unveiled an interesting discovery: models trained on skeletal-based gesture movement data can automatically generalize well to new, unseen classes without additional training. This enables the formation of compact feature spaces that establish distinguishable boundaries from old and new classes. A simple experiment on Shrec-2017 [9], as shown in Figure 3b, illustrates how within-class features cluster together, forming compact class feature spaces with minimal overlap between different classes. This phenomenon appears to be specific to skeletal data, possibly due to its structured nature. Taking a hand gesture as an example, regardless of the specific movement (e.g., pinch or swipe), all data samples are fundamentally hand motions, and the sample structure should always adhere to the physical appearance of a hand. Thus, treating all data as a single class with various subclasses, explainable by semantic relationships, seems reasonable. Previous stud-

ies [10, 12, 22, 29, 30, 32] have shown that both large image and language models demonstrated a strong relationship between feature space and semantic information, especially within a large category. Furthermore, an observation that supports this claim is the significantly higher DFCIL performance on CUB200 (lower SAD and IFM in the last session) compared to two other image datasets, as shown in Figure 2. This can possibly be attributed to the fine-grain nature of the CUB200 which contains 200 subcategories of a single large class - bird. The skeletal encoder, even trained with very limited data, appears to be capable of capturing such a feature relationship. This observation forms the basis for our feature sampling approach.

Using the mean of class feature space as class prototypes to build classifiers is a prevalent and conventional approach in FSCIL [27, 45, 53, 58]. However, relying solely on the mean may only identify a rough location within the entire feature space and is probably not sufficient to provide an accurate approximation of class feature space. Thus, in addition to the class mean μ_k , following [1, 50], we also incorporate the covariance Σ_k , providing a more comprehensive depiction of the class feature space. With the class prototype established, [50] models it as a Gaussian distribution and sample augmented features for few shot learning. Our approach also found it to be suitable for rehearsing old class data, as described in Algo. 1. By making the assumption that each class feature space follows a multivariate Gaussian distribution, we can formulate the sampling processing as:

$$(\hat{Z}_k, Y_k) | \hat{Z}_k \sim \mathcal{N}(\mu_k, \Sigma_k), \forall Y_k \in \mathcal{C}, \quad (2)$$

where \hat{Z}_k is the synthetic features space of class Y_k sampled from the distribution, \mathcal{C} is the label space.

Algorithm 1: Synthetic Feature Replay

Input: Training features from previous session
 $S_{i-1} = (Z_k, Y_k) : Y_k \in \mathcal{C}_{i-1}$, pre-trained classifier \mathcal{H}_{i-1}

- 1 **for** $Y_k \in \mathcal{C}_{i-1}$ **do**
- 2 Filtered features Z_k
 $= \{z_k \mid z_k \in Z_k, y_k = \mathcal{H}_{i-1}(z_k)\}$; #reject features if $y_k \neq \mathcal{H}_{i-1}(z_k)$;
- 3 Compute the mean $\mu_k = \mathbb{E}[Z_k]$ and the covariance $\Sigma_k = \mathbb{E}Z_k - \mu_k^T$;
- 4 [Optional] **if** Σ_k is not PSD **then**
- 5 $Z_k, u_k = \text{SVD}(Z_k)$ #reduce dimension ;
- 6 Recompute the mean and the covariance on reduced dimension space
- 7 Sample synthetic features \hat{Z}_k from μ_k and Σ_k using Eq. (2) ;
- 8 [Optional] **if** Σ_k is reduced **then**
- 9 $\hat{Z}_k = \hat{Z}_k * u_k$ # revert it back ;
- 10 Filtered synthetic features \hat{Z}_k
 $= \{\hat{z}_k \mid \hat{z}_k \in \hat{Z}_k, y_k = \mathcal{H}_{i-1}(\hat{z}_k)\}$ #reject features if $y_k \neq \mathcal{H}_{i-1}(\hat{z}_k)$;

Considering that feature representations often reside in high-dimensional spaces, a potential issue arises with the dimensionality-collapse problem. This arises when the computed class covariance fails to be positive semi-definite, contradicting the assumption of a normal distribution. One proposed solution is to employ singular value decomposition (SVD) to reduce the dimensionality of the feature space. Subsequently, sampling can be conducted in this reduced feature space, followed by reverting the sampled features back to their original dimension size, as elaborated in Algo. 1.

As shown in Figure 3a, it is evident that there is a nearly complete overlap, suggesting that the sampled features accurately mirror the feature space of the ground truth class. Thus, it comes naturally that the classifier trained with such good features can achieve excellent performance.

4.1. Effect of Supervised Contrastive learning

In contrastive learning framework, a model is trained by pulling together samples from the same classes in embedding space while pushing apart samples coming from different classes. Model trained with constraine learning are proven to generate more robust and generalizable representation, making it effective for multiple downstream tasks, and have a superior transfer ability than its cross-entropy counterpart [18]. Some previous work has shown its effectiveness in continual learning studies [11, 40].

Therefore, during the pre-training stage, we experi-

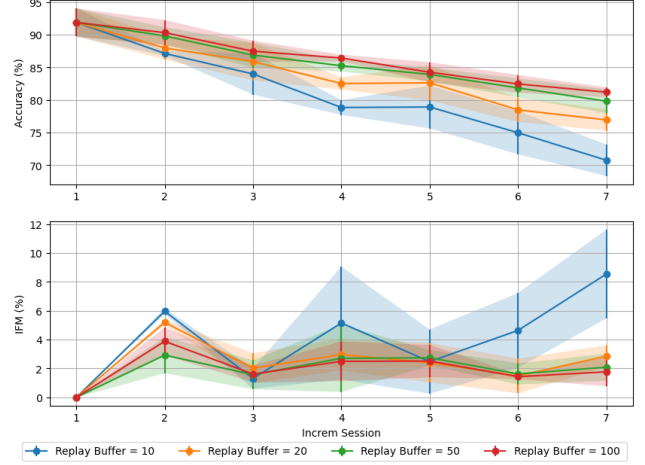


Figure 4. The impact of replay buffer size on performance when evaluating on Shrec-2017. Detailed results can be found in appendix.

mented with both vanilla cross-entropy loss and supervised contrastive loss. The supervised contrastive loss for a pair of samples (x_i, y_i) and (x_j, y_j) can be represented as:

$$\mathcal{L}_i^{Supcon} = \sum_{\substack{j=1 \\ y_i=y_j}}^N -\log \frac{\exp(z_i \cdot z_j / \tau)}{\sum_{k=1}^N \mathbb{I}_{[k=i]} \exp(z_i \cdot z_k / \tau)}. \quad (3)$$

Tables 1 and 2 show the performance when the base model is trained with Supcon and cross entropy. For Shrec-2017, which is a small dataset, the model trained with Supcon indicates a great performance for both overall accuracy and more significantly for the IFM score, which is half compared to model trained with cross entropy. However, for the much larger Ego-Gesture3D, the significance of contrastive learning is not significant.

4.2. Effect of Replay Buffer Size

We investigated how the size of synthetic features sampled affect the performance. As shown in Figure 4, performance improves as the buffer size increases from 10 to 20, 50, and nearly saturates at 100. A limited replay buffer size also results in unstable outcomes across different trials, leading to an increased standard error. This highlights the necessity of class prototypes described by mean and covariance, allowing for the sampling of more diverse examples.

4.3. SOTA Comparison

Although TEEN [45] is primarily designed for FSCIL, we re-implemented this metric learning approach for our set-up based on our observation, found that it performs well and already surpasses the SOTA previously established by BOAT-MI [1]. As shown in Figure 5, our proposed approach further improves the score, especially by achieving

Table 1. Results (average of 3 runs with different class order) for data free class-incremental learning over six tasks in Shrec-2017. SFR-CE indicates that the base model is trained using cross-entropy, while SFR-CL indicates that the base model is trained using supervised contrastive loss.

Method	Task 0	Task 1		Task 2		Task 3		Task 4		Task 5		Task 6		Mean (Task 1 \rightarrow 6)	
Oracle	89.4														
		G \uparrow	IFM \downarrow	G \uparrow	IFM \downarrow	G \uparrow	IFM \downarrow	G \uparrow	IFM \downarrow	G \uparrow	IFM \downarrow	G \uparrow	IFM \downarrow	G \uparrow	IFM \downarrow
Base [25]	90.5	78.3	7.8	53.3	29.6	30.0	53.7	27.9	56.0	12.2	78.3	11.9	78.6	35.6	50.7
Fine tuning [25]	90.5	78.6	6.0	57.4	26.2	34.2	48.8	34.0	48.6	16.4	71.8	16.1	71.9	39.5	45.5
Feature extraction [25]	90.5	79.9	9.3	69.3	12.6	62.3	19.1	56.5	24.1	50.6	24.3	45.1	32.4	60.6	20.3
LwF [25]	90.5	79.8	9.3	64.1	20.2	31.9	50.2	29.1	53.1	13.1	76.8	11.5	79.3	38.2	48.2
LwF.MC [38]	90.5	56.0	10.9	32.6	39.5	21.8	58.5	19.3	61.6	16.7	53.3	16.1	45.4	27.1	44.9
DeepInversion [52]	90.5	79.9	4.3	65.9	14.9	53.1	29.5	49.5	32.8	34.2	47.7	32.1	49.7	52.5	29.8
ABD [38]	90.5	78.8	4.0	64.6	12.6	54.3	20.3	53.2	24.6	46.1	20.0	40.4	23.3	56.2	17.5
R-DFCIL [13]	90.5	78.7	3.3	65.5	4.5	54.4	20.5	49.8	26.9	41.5	25.0	38.6	33.3	54.8	18.9
BOAT-MI [1]	90.5	83.7	4.5	76.0	7.3	71.4	7.0	69.4	13.3	64.1	9.5	58.1	11.2	70.5	8.8
TEEN [45]	91.2	87.7	12.7	80.6	27.7	76.3	28.6	72.9	27.4	68.4	29.4	64.7	31.1	77.4	22.4
Our Approaches															
SFR-CE	91.1	89.6	2.1	87.8	3.4	85.1	2.7	83.8	2.2	81.6	3.8	79.8	5.0	85.5	2.8
SFR-CL	91.9	90.1	2.1	87.3	1.1	85.9	2.4	84.0	1.9	82.5	1.6	81.1	2.8	86.1	1.7

Table 2. Results (average of 3 runs with different class order) for data free class-incremental learning over six task in Ego-Gesture3D.

Method	Task 0		Task 1		Task 2		Task 3		Task 4		Task 5		Task 6		Mean (Task 1 → 6)	
Oracle	75.8															
		G↑	IFM↓	G↑	IFM↓	G↑	IFM↓	G↑	IFM↓	G↑	IFM↓	G↑	IFM↓	G↑	IFM↓	
Base [25]	78.1	60.4	13.5	18.9	63.3	9.3	82.4	8.0	84.3	5.9	88.5	5.9	88.3	18.1	70.0	
Fine tuning [25]	78.1	59.2	10.4	15.9	66.5	9.3	82.2	7.7	84.4	5.2	89.7	5.0	90.1	17.1	70.6	
Feature extraction [25]	78.1	69.8	14.5	60.8	17.2	51.5	30.4	46.4	33.7	41.2	39.4	36.8	42.9	51.1	29.7	
LwF [25]	78.1	69.1	0.1	43.0	27.3	18.8	67.3	11.3	78.7	6.5	87.5	6.3	87.7	25.8	58.1	
LwF.MC [38]	78.1	36.8	9.8	24.2	41.3	17.0	64.6	12.8	73.3	10.2	78.3	9.7	80.2	18.4	57.9	
DeepInversion [52]	78.1	68.1	14.1	44.3	32.2	24.7	59.2	16.2	71.2	11.6	78.8	10.0	81.0	29.1	56.1	
ABD [38]	78.1	68.8	14.8	61.1	17.1	54.3	26.2	49.0	31.1	43.2	37.5	39.0	40.6	52.6	27.9	
R-DFCIL [13]	78.1	70.3	3.0	61.4	4.1	53.2	14.9	46.1	17.8	39.2	35.0	35.2	36.3	50.9	18.5	
BOAT-MI [1]	78.1	75.3	4.6	70.9	7.3	64.0	15.1	58.6	16.3	52.3	26.8	45.8	32.2	61.2	17.1	
TEEN [45]	77.8	76.2	12.8	74.6	13.3	73.1	11.9	72.2	10.9	70.7	11.4	69.4	10.9	73.4	10.2	
Our Approaches																
SFR-CE	75.7	75.5	5.7	74.3	2.3	73.1	2.2	72.3	2.4	71.3	1.9	70.4	2.5	73.2	2.4	
SFR-CL	75.3	74.6	5.6	73.6	3.7	72.6	3.7	71.8	3.7	70.6	2.7	69.8	3.0	72.6	3.2	

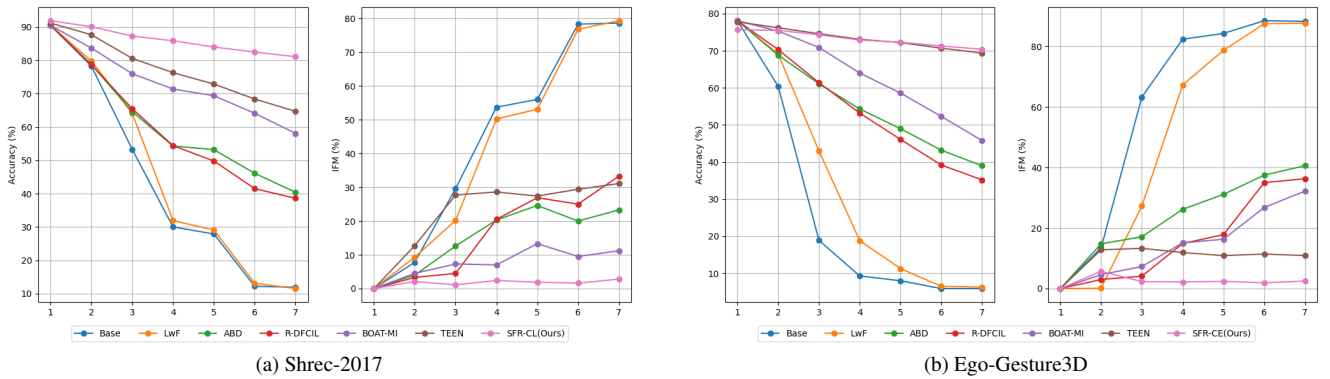


Figure 5. SOTA comparison of global accuracy and IFM for all incremental sessions.

more balanced performance (significantly lower IFM). In both data sets, the accuracy gap between two incremental sessions is impressively within 2%. For the Shrec-2017 dataset, our method shows a 16% improvement in global accuracy and a 7% reduction in IFM measures compared to

BOAT-MI. In the final and most challenging stage, our approach achieves 81% accuracy — a 23% improvement — while maintaining a very low IFM score, demonstrating an excellent accuracy balance between base and new classes. For the Ego-Gesture3D dataset, when comparing the final

Table 3. Results (average of 3 runs with different shots selected) for few shot class-incremental learning in Shrec-2017.

Method	Task 0	Task 1		Task 2		Task 3		Task 4		Task 5		Task 6		Mean (Task 1 → 6)	
		G↑	IFM↓	G↑	IFM↓	G↑	IFM↓	G↑	IFM↓	G↑	IFM↓	G↑	IFM↓	G↑	IFM↓
Full-Shot	89.4	88.4	3.3	87.3	2.1	86.0	0.5	85.3	0.2	83.0	0.2	82.3	1.9	85.9	1.2
10-Shot w/o Aug	89.4	88.0	6.2	86.3	5.8	81.8	12.1	85.4	1.2	78.8	6.9	78.9	6.2	84.1	5.5
5-Shot w/o Aug	89.4	85.9	20.7	82.8	15.8	79.9	13.2	78.5	9.8	75.9	11.1	74.4	10.1	81.0	11.5
5-Shot w/ Aug	89.4	87.2	10.0	84.2	10.5	79.2	9.7	79.8	5.9	75.0	10.2	74.4	5.9	81.3	7.5

Table 4. Results (average of 3 runs with different shots selected) for few shot class-incremental learning in Ego-Gesture3D.

Method	Task 0	Task 1		Task 2		Task 3		Task 4		Task 5		Task 6		Mean (Task 1 → 6)	
		G↑	IFM↓	G↑	IFM↓	G↑	IFM↓	G↑	IFM↓	G↑	IFM↓	G↑	IFM↓	G↑	IFM↓
Full-Shot	75.2	75.6	2.5	73.1	3.0	72.7	1.7	72.7	2.4	70.2	2.2	69.5	3.2	72.7	2.1
10-Shot w/o Aug	75.2	73.6	14.5	71.8	9.0	68.9	11.5	66.5	8.1	66.3	6.5	63.0	13.6	69.4	9.0
5-Shot w/o Aug	75.2	72.1	15.8	68.4	25.2	65.1	18.6	64.4	15.2	60.8	19.3	58.9	20.2	66.4	16.3
5-Shot w/ Aug	75.2	72.3	10.8	69.1	14.2	66.6	15.7	66.4	12.5	62.6	11.9	58.3	18.0	67.2	11.9

step accuracy after training on all classes to the oracle setup in which the model is trained on all classes simultaneously, there is only a 5% decline, which is impressive among conventional DFCIL tasks. Previous approaches testing on image datasets typically suffered from significant accuracy imbalances between new and old classes, indicated by high IFM scores that worsen with continued incremental learning. Our approach significantly mitigates this effect, keeping the IFM within 5% for all incremental sessions in both tested datasets.

5. Few-Shot Class Incremental Learning

In the real world, the number of samples that the user can provide to update the model is usually limited. For instance, if the user would like to register a personalized gesture, it is crucial to balance the need for data with the user experience, as asking for too much data can be burdensome and discourage users from using the developed function. Therefore, while our primary focus is on DFCIL, we also examine our approach within FSCIL to evaluate its performance with limited data availability.

5.1. Effect of Shot Size

To investigate the impact of sample size on the performance, we conducted experiments across three settings, 5-Shot, 10-Shot, and Full-Shot. The comparison results are presented in Tables 3 and 4. We can easily see that, for both datasets, having a larger sample size can significantly improve the performance, particularly for IFM. For Shrec-2017 dataset, employing a 5-Shot setup results in a roughly 9% decrease in accuracy and yields a significantly higher IFM score, increasing from 2% to 13.2%, compared to the Full-Shot setup. This phenomenon contrasts with many other frozen encoder-based approaches that achieve SOTA performance on image datasets. For example, [53] shows marginal or even slightly worse performance with increased data availability.

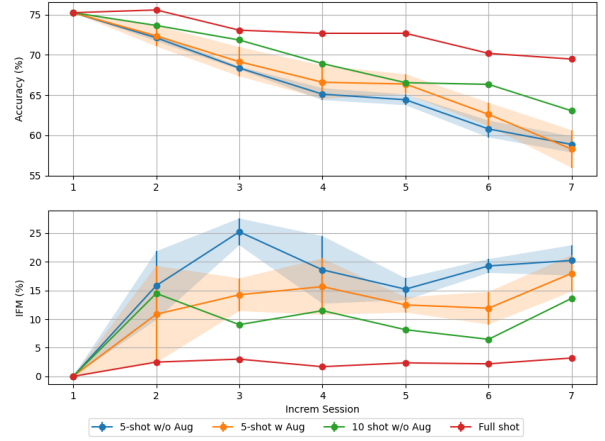


Figure 6. The effect of shot size and augmentation on Ego-Gesture3D. Both the blue and orange lines indicate the 5-Shot setting with the orange lines denotes the synthetic feature augmentation enabled.

We attributed the positive relation between shot size and performance mainly to our design of employing prototypes constructed by mean and covariance. With more training data, there is a greater likelihood of uncovering the true and robust class distribution without being influenced by outliers or unrepresentative samples. Consequently, this allows for the generation of more diverse yet still within-distribution synthetic features.

5.2. Feature Augmentation

In light of the positive relationship between performance and the size of training samples, the instinctive approach is to augment or generate additional synthetic features for classifier training [50]. However, using fewer samples to construct prototypes increases the likelihood of biasing the simulated class distribution away from the true distribution. Then, the problem becomes how can we sample the correct features from a likely biased distribution. In the feature replay method previously outlined, where the classifier

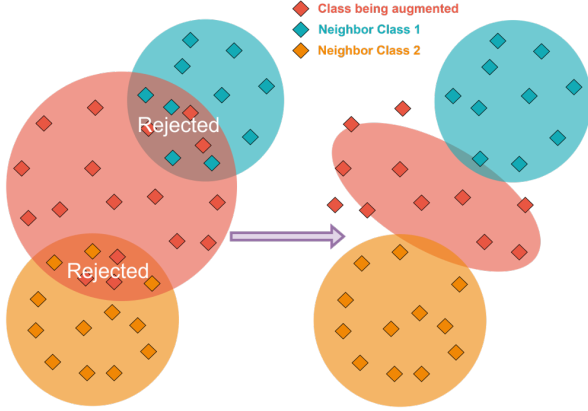


Figure 7. Illustration of sampling process for augmentation. (1) Naively sample enough features from class prototype obtained from real features (limited in few shot setting). (2) Reconstruct the prototype by rejecting sampled features if they are too close to their neighbor class distribution. (3) Re-sampling features from the calibrated prototype for augmentation.

trained for the previous step is available, candidate features can be inputted into the previous classifier, and samples that cannot be classified correctly are rejected.

However, the purpose now shifts towards learning the newly introduced classes instead of replaying for old classes. Thus, we developed a sampling filter strategy to discard samples confused by multiple classes, and this strategy is grounded in the assumption that the ground truth feature space for each class is compact and distinguishable, which we have reason to believe based on the earlier observation. This process involves utilizing Mahalanobis Distance D_M to measure the distance between each sampled feature and the feature distribution of other classes. Samples are rejected if the distance falls below a threshold β . After that, we reconstruct the calibrated feature space from the filtered synthetic features, allowing us to sample new and more robust synthetic features, as described in Algo. 2.

$$D_M = \sqrt{(\mathbf{z} - \mu)^\top \sigma^{-1} (\mathbf{z} - \mu)}. \quad (4)$$

We investigate the impact of our proposed feature augmentation for new classes in the 5-shot setting. As shown in Figure. 6, with our proposed augmentation approach, there is an improvement in both global accuracy and IFM consistent across all incremental sessions.

6. Experiments

6.1. Dataset

Following the experimental protocol established by BOAT-MI [1], we evaluated our approaches on two hand gesture skeleton datasets, **Shrec-2017** [9] and **Ego-Gesture3D** [1, 54]. Furthermore, we further evaluated a

Algorithm 2: Synthetic Feature Augmentation

Input: Training features $S_i = (Z_k, Y_k) : Y_k \in \mathcal{C}_i$,
all seen class prototypes $\mathcal{P}_j : Y_j \in \bigcup_{j=0}^{i-1} \mathcal{C}_j$

- 1 **for** $Y_k \in \mathcal{C}_i$ **do**
- 2 Compute the mean μ_k and the covariance Σ_k from Z_k ;
- 3 Sample synthetic features \hat{Z}_k from μ_k and Σ_k using Eq.2 ;
- 4 Filtered synthetic features $\hat{\hat{Z}}_k$
 $= \{\hat{z}_k \mid \hat{z}_k \in \hat{Z}_k, D_M(\hat{z}_k, \mathcal{P}_j) < \beta\}$; Here,
 $\mathcal{P}_j : j \neq i, Y_j \in \bigcup_{j=0}^{i-1} \mathcal{C}_j$ is the class
distribution for all other classes ;
- 5 Re-compute the mean $\hat{\mu}_k$ and the covariance $\hat{\Sigma}_k$;
- 6 Re-sample synthetic features $\hat{\hat{Z}}_k$ from the calibrated prototype;
- 7 $Z_k = [Z_k, \hat{\hat{Z}}_k]$ # combine fake features and real features ;

new body gesture skeleton dataset, **NTU-RGB+D** [35]. (Detailed information can be found in the appendix.)

6.2. Experiment Setup

We maintain the incremental task split consistent with BOAT-MI [1]. For the Shrec-2017 dataset, the base class size is set to 8, with 1 class added incrementally. For the Ego-Gesture3D dataset, there are 59 base classes with 4 new classes added at a time. For DFCIL, we conduct three trials for each dataset with different incremental class orders, following the approach of BOAT-MI [1]. For FSCIL, we perform three trials with different shot selections but the same incremental class order. Unlike some existing FSCIL methods that run only a single trial, we emphasize the importance of multiple runs. As shown in Table 6, the standard deviation of the metrics can exceed 15% in all trials, particularly when the shot size is limited, making the impact of outliers significant.

7. Conclusion

DFCIL for gesture recognition has big real-world implications. In this study, we observe skeletons inherently possess a greater generalization ability to new classes and therefore propose a synthetic feature sampling strategy that can replay old class data and augment new class data. Compared to previous approaches, our method not only achieves greater performance, but is also much more efficient, better suited for the gesture recognition domain, which primarily operates on edge devices.

References

- [1] Shubhra Aich, Jesus Ruiz-Santaquiteria, Zhenyu Lu, Prachi Garg, KJ Joseph, Alvaro Fernandez Garcia, Vineeth N Balasubramanian, Kenrick Kin, Chengde Wan, Necati Cihan Camgoz, et al. Data-free class-incremental hand gesture recognition. In *Proceedings of the IEEE/CVF International Conference on Computer Vision*, pages 20958–20967, 2023. 2, 3, 4, 5, 6, 8
- [2] Shubhra Aich, Jesus Ruiz-Santaquiteria, Zhenyu Lu, Prachi Garg, K J Joseph, Alvaro Fernandez Garcia, Vineeth N Balasubramanian, Kenrick Kin, Chengde Wan, Necati Cihan Camgoz, Shugao Ma, and Fernando De la Torre. Data-free class-incremental hand gesture recognition. In *Proceedings of the IEEE/CVF International Conference on Computer Vision (ICCV)*, pages 20958–20967, October 2023. 3
- [3] Afra Feyza Akyürek, Ekin Akyürek, Derry Tanti Wijaya, and Jacob Andreas. Subspace regularizers for few-shot class incremental learning. *arXiv preprint arXiv:2110.07059*, 2021. 2
- [4] Mathilde Caron, Hugo Touvron, Ishan Misra, Hervé Jégou, Julien Mairal, Piotr Bojanowski, and Armand Joulin. Emerging properties in self-supervised vision transformers. In *Proceedings of the IEEE/CVF international conference on computer vision*, pages 9650–9660, 2021. 1
- [5] Francisco M Castro, Manuel J Marín-Jiménez, Nicolás Guil, Cordelia Schmid, and Karteek Alahari. End-to-end incremental learning. In *Proceedings of the European conference on computer vision (ECCV)*, pages 233–248, 2018. 2
- [6] Yuxiao Chen, Long Zhao, Xi Peng, Jianbo Yuan, and Dimitris N Metaxas. Construct dynamic graphs for hand gesture recognition via spatial-temporal attention. *arXiv preprint arXiv:1907.08871*, 2019. 2
- [7] Hyung-gun Chi, Myoung Hoon Ha, Seunggeun Chi, Sang Wan Lee, Qixing Huang, and Karthik Ramani. Infogcn: Representation learning for human skeleton-based action recognition. In *Proceedings of the IEEE/CVF conference on computer vision and pattern recognition*, pages 20186–20196, 2022. 2
- [8] Yulai Cong, Miaoyun Zhao, Jianqiao Li, Sijia Wang, and Lawrence Carin. Gan memory with no forgetting. *Advances in Neural Information Processing Systems*, 33:16481–16494, 2020. 1, 2, 3
- [9] Quentin De Smedt, Hazem Wannous, J-P Vandeborrel, Joris Guerry, B Le Saux, and David Filliat. 3d hand gesture recognition using a depth and skeletal dataset: Shrec’17 track. In *Proceedings of the Workshop on 3D Object Retrieval*, pages 33–38, 2017. 4, 8
- [10] Ali Farhadi, Ian Endres, Derek Hoiem, and David Forsyth. Describing objects by their attributes. In *2009 IEEE conference on computer vision and pattern recognition*, pages 1778–1785. IEEE, 2009. 4
- [11] Enrico Fini, Victor G Turrissi Da Costa, Xavier Alameda-Pineda, Elisa Ricci, Karteek Alahari, and Julien Mairal. Self-supervised models are continual learners. In *Proceedings of the IEEE/CVF Conference on Computer Vision and Pattern Recognition*, pages 9621–9630, 2022. 5
- [12] Andrea Frome, Greg S Corrado, Jon Shlens, Samy Bengio, Jeff Dean, Marc’ Aurelio Ranzato, and Tomas Mikolov. Devise: A deep visual-semantic embedding model. *Advances in neural information processing systems*, 26, 2013. 4
- [13] Qiankun Gao, Chen Zhao, Bernard Ghanem, and Jian Zhang. R-dfcil: Relation-guided representation learning for data-free class incremental learning. In *European Conference on Computer Vision*, pages 423–439. Springer, 2022. 2, 3, 6
- [14] Spyros Gidaris and Nikos Komodakis. Dynamic few-shot visual learning without forgetting. In *Proceedings of the IEEE conference on computer vision and pattern recognition*, pages 4367–4375, 2018. 2
- [15] Shangchen Han, Beibei Liu, Randi Cabezas, Christopher D Twigg, Peizhao Zhang, Jeff Petkau, Tsz-Ho Yu, Chun-Jung Tai, Muzaffer Akbay, Zheng Wang, et al. Megatrack: monochrome egocentric articulated hand-tracking for virtual reality. *ACM Transactions on Graphics (ToG)*, 39(4):87–1, 2020. 2
- [16] Shangchen Han, Po-chen Wu, Yubo Zhang, Beibei Liu, Linguang Zhang, Zheng Wang, Weiguang Si, Peizhao Zhang, Yujun Cai, Tomas Hodan, et al. Umetrack: Unified multi-view end-to-end hand tracking for vr. In *SIGGRAPH Asia 2022 Conference Papers*, pages 1–9, 2022. 2
- [17] Saihui Hou, Xinyu Pan, Chen Change Loy, Zilei Wang, and Dahua Lin. Learning a unified classifier incrementally via rebalancing. In *Proceedings of the IEEE/CVF conference on computer vision and pattern recognition*, pages 831–839, 2019. 2
- [18] Ashraful Islam, Chun-Fu Richard Chen, Rameswar Panda, Leonid Karlinsky, Richard Radke, and Rogerio Feris. A broad study on the transferability of visual representations with contrastive learning. In *Proceedings of the IEEE/CVF International Conference on Computer Vision*, pages 8845–8855, 2021. 5
- [19] Alexander Kirillov, Eric Mintun, Nikhila Ravi, Hanzi Mao, Chloe Rolland, Laura Gustafson, Tete Xiao, Spencer Whitehead, Alexander C Berg, Wan-Yen Lo, et al. Segment anything. In *Proceedings of the IEEE/CVF International Conference on Computer Vision*, pages 4015–4026, 2023. 1
- [20] James Kirkpatrick, Razvan Pascanu, Neil Rabinowitz, Joel Veness, Guillaume Desjardins, Andrei A Rusu, Kieran Milan, John Quan, Tiago Ramalho, Agnieszka Grabska-Barwinska, et al. Overcoming catastrophic forgetting in neural networks. *Proceedings of the national academy of sciences*, 114(13):3521–3526, 2017. 2
- [21] Anna Kukleva, Hilde Kuehne, and Bernt Schiele. Generalized and incremental few-shot learning by explicit learning and calibration without forgetting. In *Proceedings of the IEEE/CVF international conference on computer vision*, pages 9020–9029, 2021. 2
- [22] Christoph H Lampert, Hannes Nickisch, and Stefan Harmeling. Learning to detect unseen object classes by between-class attribute transfer. In *2009 IEEE conference on computer vision and pattern recognition*, pages 951–958. IEEE, 2009. 4
- [23] Jungho Lee, Minhyeok Lee, Dogyoon Lee, and Sangyoun Lee. Hierarchically decomposed graph convolutional networks for skeleton-based action recognition. In *Proceedings*

- of the *IEEE/CVF International Conference on Computer Vision*, pages 10444–10453, 2023. 2
- [24] Kibok Lee, Kimin Lee, Jinwoo Shin, and Honglak Lee. Overcoming catastrophic forgetting with unlabeled data in the wild. In *Proceedings of the IEEE/CVF International Conference on Computer Vision*, pages 312–321, 2019.
- [25] Zhizhong Li and Derek Hoiem. Learning without forgetting. *IEEE transactions on pattern analysis and machine intelligence*, 40(12):2935–2947, 2017. 1, 2, 6
- [26] Huan Liu, Li Gu, Zhixiang Chi, Yang Wang, Yuanhao Yu, Jun Chen, and Jin Tang. Few-shot class-incremental learning via entropy-regularized data-free replay. In *European Conference on Computer Vision*, pages 146–162. Springer, 2022. 3
- [27] Jinlu Liu, Liang Song, and Yongqiang Qin. Prototype rectification for few-shot learning. In *Computer Vision–ECCV 2020: 16th European Conference, Glasgow, UK, August 23–28, 2020, Proceedings, Part I 16*, pages 741–756. Springer, 2020. 2, 4
- [28] Michael McCloskey and Neal J Cohen. Catastrophic interference in connectionist networks: The sequential learning problem. In *Psychology of learning and motivation*, volume 24, pages 109–165. Elsevier, 1989. 2
- [29] Tomas Mikolov, Kai Chen, Greg Corrado, and Jeffrey Dean. Efficient estimation of word representations in vector space. *arXiv preprint arXiv:1301.3781*, 2013. 4
- [30] Mohammad Norouzi, Tomas Mikolov, Samy Bengio, Yoram Singer, Jonathon Shlens, Andrea Frome, Greg S Corrado, and Jeffrey Dean. Zero-shot learning by convex combination of semantic embeddings. *arXiv preprint arXiv:1312.5650*, 2013. 4
- [31] Juan C Nunez, Raul Cabido, Juan J Pantrigo, Antonio S Montemayor, and Jose F Velez. Convolutional neural networks and long short-term memory for skeleton-based human activity and hand gesture recognition. *Pattern Recognition*, 76:80–94, 2018. 2
- [32] Mark Palatucci, Dean Pomerleau, Geoffrey E Hinton, and Tom M Mitchell. Zero-shot learning with semantic output codes. *Advances in neural information processing systems*, 22, 2009. 4
- [33] Alec Radford, Jong Wook Kim, Chris Hallacy, Aditya Ramesh, Gabriel Goh, Sandhini Agarwal, Girish Sastry, Amanda Askell, Pamela Mishkin, Jack Clark, et al. Learning transferable visual models from natural language supervision. In *International conference on machine learning*, pages 8748–8763. PMLR, 2021. 1
- [34] Sylvestre-Alvise Rebuffi, Alexander Kolesnikov, Georg Sperl, and Christoph H Lampert. icarl: Incremental classifier and representation learning. In *Proceedings of the IEEE conference on Computer Vision and Pattern Recognition*, pages 2001–2010, 2017. 1, 2
- [35] Amir Shahroudy, Jun Liu, Tian-Tsong Ng, and Gang Wang. Ntu rgb+ d: A large scale dataset for 3d human activity analysis. In *Proceedings of the IEEE conference on computer vision and pattern recognition*, pages 1010–1019, 2016. 8
- [36] Lei Shi, Yifan Zhang, Jian Cheng, and Hanqing Lu. Decoupled spatial-temporal attention network for skeleton-based action-gesture recognition. In *Proceedings of the Asian conference on computer vision*, 2020. 2
- [37] Hanul Shin, Jung Kwon Lee, Jaehong Kim, and Jiwon Kim. Continual learning with deep generative replay. *Advances in neural information processing systems*, 30, 2017. 2, 3
- [38] James Smith, Yen-Chang Hsu, Jonathan Balloch, Yilin Shen, Hongxia Jin, and Zsolt Kira. Always be dreaming: A new approach for data-free class-incremental learning. In *Proceedings of the IEEE/CVF International Conference on Computer Vision*, pages 9374–9384, 2021. 2, 6
- [39] Jake Snell, Kevin Swersky, and Richard Zemel. Prototypical networks for few-shot learning. *Advances in neural information processing systems*, 30, 2017. 2
- [40] Zeyin Song, Yifan Zhao, Yujun Shi, Peixi Peng, Li Yuan, and Yonghong Tian. Learning with fantasy: Semantic-aware virtual contrastive constraint for few-shot class-incremental learning. In *Proceedings of the IEEE/CVF conference on computer vision and pattern recognition*, pages 24183–24192, 2023. 2, 5
- [41] Xiaoyu Tao, Xiaopeng Hong, Xinyuan Chang, Songlin Dong, Xing Wei, and Yihong Gong. Few-shot class-incremental learning. In *Proceedings of the IEEE/CVF conference on computer vision and pattern recognition*, pages 12183–12192, 2020. 1, 2
- [42] Fu-Yun Wang, Da-Wei Zhou, Liu Liu, Han-Jia Ye, Yatao Bian, De-Chuan Zhan, and Peilin Zhao. Beef: Bi-compatible class-incremental learning via energy-based expansion and fusion. In *The eleventh international conference on learning representations*, 2022. 2
- [43] Fu-Yun Wang, Da-Wei Zhou, Han-Jia Ye, and De-Chuan Zhan. Foster: Feature boosting and compression for class-incremental learning. In *European conference on computer vision*, pages 398–414. Springer, 2022. 2
- [44] Lei Wang and Piotr Koniusz. 3mformer: Multi-order multi-mode transformer for skeletal action recognition. In *Proceedings of the IEEE/CVF Conference on Computer Vision and Pattern Recognition*, pages 5620–5631, 2023. 2
- [45] Qi-Wei Wang, Da-Wei Zhou, Yi-Kai Zhang, De-Chuan Zhan, and Han-Jia Ye. Few-shot class-incremental learning via training-free prototype calibration. *Advances in Neural Information Processing Systems*, 36, 2024. 2, 3, 4, 5, 6
- [46] Yue Wu, Yinpeng Chen, Lijuan Wang, Yuancheng Ye, Zicheng Liu, Yandong Guo, and Yun Fu. Large scale incremental learning. In *Proceedings of the IEEE/CVF conference on computer vision and pattern recognition*, pages 374–382, 2019. 2
- [47] Tianjun Xiao, Jiaxing Zhang, Kuiyuan Yang, Yuxin Peng, and Zheng Zhang. Error-driven incremental learning in deep convolutional neural network for large-scale image classification. In *Proceedings of the 22nd ACM international conference on Multimedia*, pages 177–186, 2014. 2
- [48] Shipeng Yan, Jiangwei Xie, and Xuming He. Der: Dynamically expandable representation for class incremental learning. In *Proceedings of the IEEE/CVF conference on computer vision and pattern recognition*, pages 3014–3023, 2021. 2
- [49] Sijie Yan, Yuanjun Xiong, and Dahua Lin. Spatial temporal graph convolutional networks for skeleton-based action

- recognition. In *Proceedings of the AAAI conference on artificial intelligence*, volume 32, 2018. 2
- [50] Shuo Yang, Lu Liu, and Min Xu. Free lunch for few-shot learning: Distribution calibration. *arXiv preprint arXiv:2101.06395*, 2021. 4, 7
 - [51] Yang Yang, Da-Wei Zhou, De-Chuan Zhan, Hui Xiong, and Yuan Jiang. Adaptive deep models for incremental learning: Considering capacity scalability and sustainability. In *Proceedings of the 25th ACM SIGKDD International Conference on Knowledge Discovery & Data Mining*, pages 74–82, 2019. 1, 2
 - [52] Hongxu Yin, Pavlo Molchanov, Jose M Alvarez, Zhizhong Li, Arun Mallya, Derek Hoiem, Niraj K Jha, and Jan Kautz. Dreaming to distill: Data-free knowledge transfer via deep-inversion. In *Proceedings of the IEEE/CVF Conference on Computer Vision and Pattern Recognition*, pages 8715–8724, 2020. 2, 3, 6
 - [53] Chi Zhang, Nan Song, Guosheng Lin, Yun Zheng, Pan Pan, and Yinghui Xu. Few-shot incremental learning with continually evolved classifiers. In *Proceedings of the IEEE/CVF conference on computer vision and pattern recognition*, pages 12455–12464, 2021. 2, 3, 4, 7
 - [54] Yifan Zhang, Congqi Cao, Jian Cheng, and Hanqing Lu. Egogesture: a new dataset and benchmark for egocentric hand gesture recognition. *IEEE Transactions on Multimedia*, 20(5):1038–1050, 2018. 8
 - [55] Yuhan Zhang, Bo Wu, Wen Li, Lixin Duan, and Chuang Gan. Stst: Spatial-temporal specialized transformer for skeleton-based action recognition. In *Proceedings of the 29th ACM International Conference on Multimedia*, pages 3229–3237, 2021. 2
 - [56] Da-Wei Zhou, Fu-Yun Wang, Han-Jia Ye, Liang Ma, Shiliang Pu, and De-Chuan Zhan. Forward compatible few-shot class-incremental learning. In *Proceedings of the IEEE/CVF conference on computer vision and pattern recognition*, pages 9046–9056, 2022. 2
 - [57] Da-Wei Zhou, Han-Jia Ye, Liang Ma, Di Xie, Shiliang Pu, and De-Chuan Zhan. Few-shot class-incremental learning by sampling multi-phase tasks. *IEEE Transactions on Pattern Analysis and Machine Intelligence*, 2022. 2, 3
 - [58] Kai Zhu, Yang Cao, Wei Zhai, Jie Cheng, and Zheng-Jun Zha. Self-promoted prototype refinement for few-shot class-incremental learning. In *Proceedings of the IEEE/CVF conference on computer vision and pattern recognition*, pages 6801–6810, 2021. 2, 4

Supplementary Materials: Data-Free Class Incremental Gesture Recognition via Synthetic Feature Samplings

Anonymous WACV Algorithms Track submission

Paper ID 900

1. Experiment Details

1.1. Datasets

We employ three skeleton datasets for experiments, detailed as follows:

Shrec-2017 [?] comprises of 14 coarse and fine-grained gestures with a training-validation and testing sets of 1980 and 840 samples from a disjoint set of 20 and 8 subjects, respectively.

Ego-Gesture3D is the 3D skeletal version of the Ego-Gesture [?]. Its original RGB-D dataset contains 14416 training, 4768 validation, and 4977 test samples and there are 83 gesture classes in total. BOAT-MI [?] constructed its skeletal version through using MediaPipe [?] to extract 3D skeletons.

NTU-RGB+D [?] is a large human action dataset and comprises of 56880 samples of 60 action classless collected from 40 subjects. It provides multi-modality information including depth images, 3D skeleton, RGB frames, and infrared sequences and we used skeleton modality only. The task split is defined as a combination of 36 base classes and remaining 24 classes equally divided into 6 incremental sessions. Similarly, three trials with different class orders are evaluated.

Image datasets are out of our scope, but we reproduced TEEN [?] on the following three datasets to investigate the overall DFCIL performance difference between image and skeleton datasets. Our subset split exactly follows the previous methods [?].

CIFAR-100 [?] compromises of 60000 color images of 100 classes. There are 500 training images and 100 testing images per class. The whole dataset is divided into 60 base classes and the remaining 40 classes are divided into 8 incremental sessions.

CUB-200 [?] compromises of 11788 color images of 200 classes all belonging to birds and is widely used for fine-grained visual categorization task. There are 5994 training images and 5794 testing images. The whole dataset is di-

vided into 100 base classes and the remaining 100 classes are divided into 10 incremental sessions.

MiniImageNet [?] is sampled from the raw ImageNet and compromises of 50000 training images and 10000 testing images, evenly distributed across 100 classes. The whole dataset is divided into 60 base classes and the remaining 40 classes are divided into 8 incremental sessions.

1.2. Implementation Details

Following BOAT-MI [?], we utilize the DG-STA [?] architecture as our base model for Shrec-2017 and Ego-Gesture3D with a frame length of 8 and a batch size of 64. The base model is trained with either cross-entropy and supervised contrastive loss, with Adam optimizer ($\text{lr} = 1\text{e-}3$, $\beta_1 = 0.9$ and $\beta_2 = 0.999$) for 100 epochs. We utilize a simple linear layer as our classification head, and the linear layer is trained with Adam optimizer ($\text{lr} = 1\text{e-}1$, $\beta_1 = 0.9$ and $\beta_2 = 0.999$) for 50 epochs and the best model is selected for evaluation.

For NTU, we utilize the ST-GCN [?] as our base model with a frame length of 100 and a batch size of 32. The training detail is the same as above except the base model is trained for 50 epochs instead.

The synthetic feature size for both replay and augmentation is set to 100 per class with an initial candidate pool size of 300, followed by filtering and then randomly picking 100 as the final feature pool. A dataset can be constructed with all the synthetic features and is replayed/augmented with sample size $= \alpha$ times the newly introduced data batch size for each iteration in a rolling way. The hyper-parameter α is selected to be 8.

The training details of TEEN on image datasets exactly follows their setup, except all training data are used instead of 5 samples per class.

The threshold β for synthetic feature augmentation used in FSCIL is initially set to 30 and the rest set up is the same as in DFCIL. If the target size of sampled feature can't be met after filtering, we can iteratively reduce the β until sufficient features are sampled.

Table 1. Comparison of DFCIL performance with different size of replay buffer in Shrec-2017

	Task 0	Task 1		Task 2		Task 3		Task 4		Task 5		Task 6		Mean (Task 1 → 6)	
Buffer Size		G↑	IFM↓	G↑	IFM↓	G↑	IFM↓	G↑	IFM↓	G↑	IFM↓	G↑	IFM↓	G↑	IFM↓
10	91.9	87.1	6.0	84.0	1.3	78.8	5.1	78.9	2.5	75.0	4.6	70.8	8.5	80.9	4.0
20	91.9	88.0	5.2	85.9	2.0	82.5	3.0	82.6	2.4	78.5	1.5	76.9	2.9	83.8	2.4
50	91.9	89.8	2.9	86.9	1.6	85.3	2.7	83.9	2.7	81.8	1.6	79.8	2.1	85.6	2.0
100	91.9	90.3	3.9	87.5	1.6	86.4	2.5	84.2	2.5	82.5	1.4	81.2	1.8	86.3	2.0

Table 2. Results of TEEN for data free class-incremental learning over six tasks in Image datasets.

Method	Task 0	Task 1		Task 2		Task 3		Task 4		Task 5		Task 6		Mean (Task 1 → 6)	
		G↑	IFM↓	G↑	IFM↓	G↑	IFM↓	G↑	IFM↓	G↑	IFM↓	G↑	IFM↓	G↑	IFM↓
CIFAR100 [?]	75.5	72.2	13.5	69.1	18.0	65.9	21.2	63.4	21.6	61.0	20.4	59.5	18.7	66.7	16.2
CUB200 [?]	79.4	75.2	7.0	73.5	9.3	69.6	14.2	70.8	9.4	68.2	9.2	69.6	7.1	72.3	8.0
MiniImageNet [?]	75.3	70.8	10.1	68.2	11.7	65.7	12.6	63.7	12.0	62.2	12.1	60.2	12.7	66.6	10.2

Table 3. Results (average of 3 runs with different class order) for data free class-incremental learning over six tasks in NTU

Method	Task 0	Task 1		Task 2		Task 3		Task 4		Task 5		Task 6		Mean (Task 1 → 6)	
		G↑	IFM↓	G↑	IFM↓	G↑	IFM↓	G↑	IFM↓	G↑	IFM↓	G↑	IFM↓	G↑	IFM↓
TEEN	88.6	84.4	15.5	81.4	15.0	78.6	14.0	76.6	13.3	72.8	15.0	70.7	14.2	79.0	12.4
SFR-CE	87.9	80.9	3.4	79.4	1.8	78.1	0.7	76.1	2.2	74.3	3.2	71.8	2.4	78.4	1.9
SFR-CL	84.3	79.9	5.1	80.0	1.0	77.8	0.6	77.0	1.5	74.4	2.9	72.9	2.7	78.0	2.0

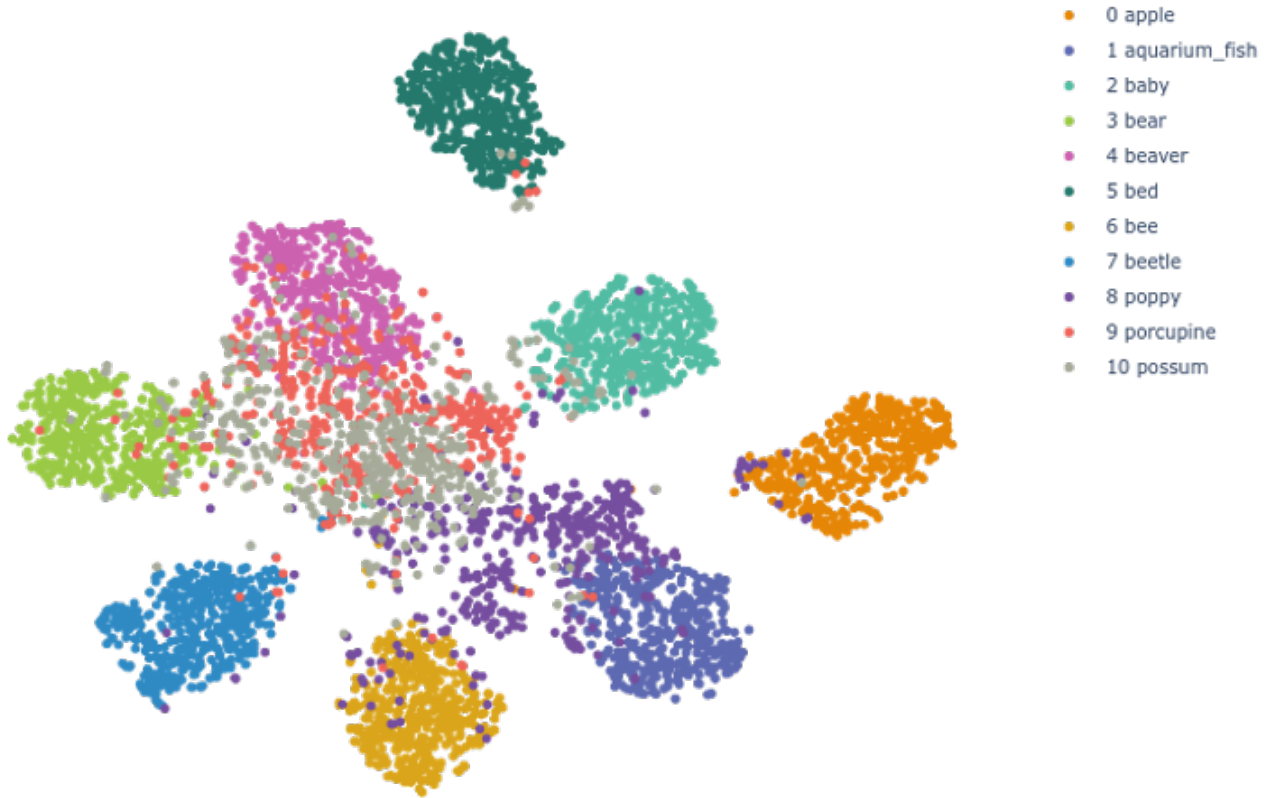


Figure 1. A toy experiment on image dataset CIFAR100, three new classes were added to a model pre-trained on eight base classes (8,9,10 are three newly introduced classes). Unlike the pattern observed in the skeleton experiment, these newly introduced image classes do not form compact and distinguishable feature spaces. As a result, there is significant overlap between the feature spaces of different classes.

216 **2. Discussion**
217
218 **Performance on body motion dataset** BOAT-MI [?] only evaluates on two hand gesture datasets, we test our
219 findings and approaches on a new body motion skeleton
220 dataset - NTU. Since BOAT-MI involves a very time con-
221 suming model inversion technique (their implementation of
222 model inversion doesn't support batch processing), it takes
223 too much time when evaluated on the much larger NTU
224 dataset. Therefore, we only compared our approach against
225 TEEN [?] which is training-free and has already shown su-
226 perior performance compared to BOAT-MI. As shown in
227 Table. 3, our approach can also adapt to human body skele-
228 ton dataset as well.
229
230
231 **Normal distribution validation** To verify the correctness
232 and feasibility of the Gaussian assumption in our approach,
233 we plot histograms and quantile-quantile (Q-Q) plots for the
234 top six principal components of the class feature space to vi-
235 sually inspect the distribution of the feature space as shown
236 in Fig.2. In most cases, the histograms exhibit strong Gaus-
237 sian characteristics, and the Q-Q plots largely align with the
238 identity line. This indicates that modeling the class feature
239 space as a Gaussian distribution is reasonable. However,
240 some samples are concentrated in the tails as well, forming
241 a tailed distribution. For future work, incorporating a prior
242 to ensure that the features of an encoder follow a normal
243 distribution could be a potential solution.
244
245 **Combine with other approaches** Our approach doesn't
246 involve any special training or fine-tuning design of the en-
247 coder. This allows it to be easily integrated with other meth-
248 ods to further enhance performance. It can be combined
249 with improved training strategies for the base model, such
250 as FACT [?], SAVC [?] or fine-tuning techniques for better
251 adaptation to newly introduced classes.
252
253
254
255
256
257
258
259
260
261
262
263
264
265
266
267
268
269

270
271
272
273
274
275
276
277
278
279
280
281
282
283
284
285
286
287
288
289
290
291
292
293
294
295
296
297
298
299
300
301
302
303
304
305
306
307
308
309
310
311
312
313
314
315
316
317
318
319
320
321
322
323

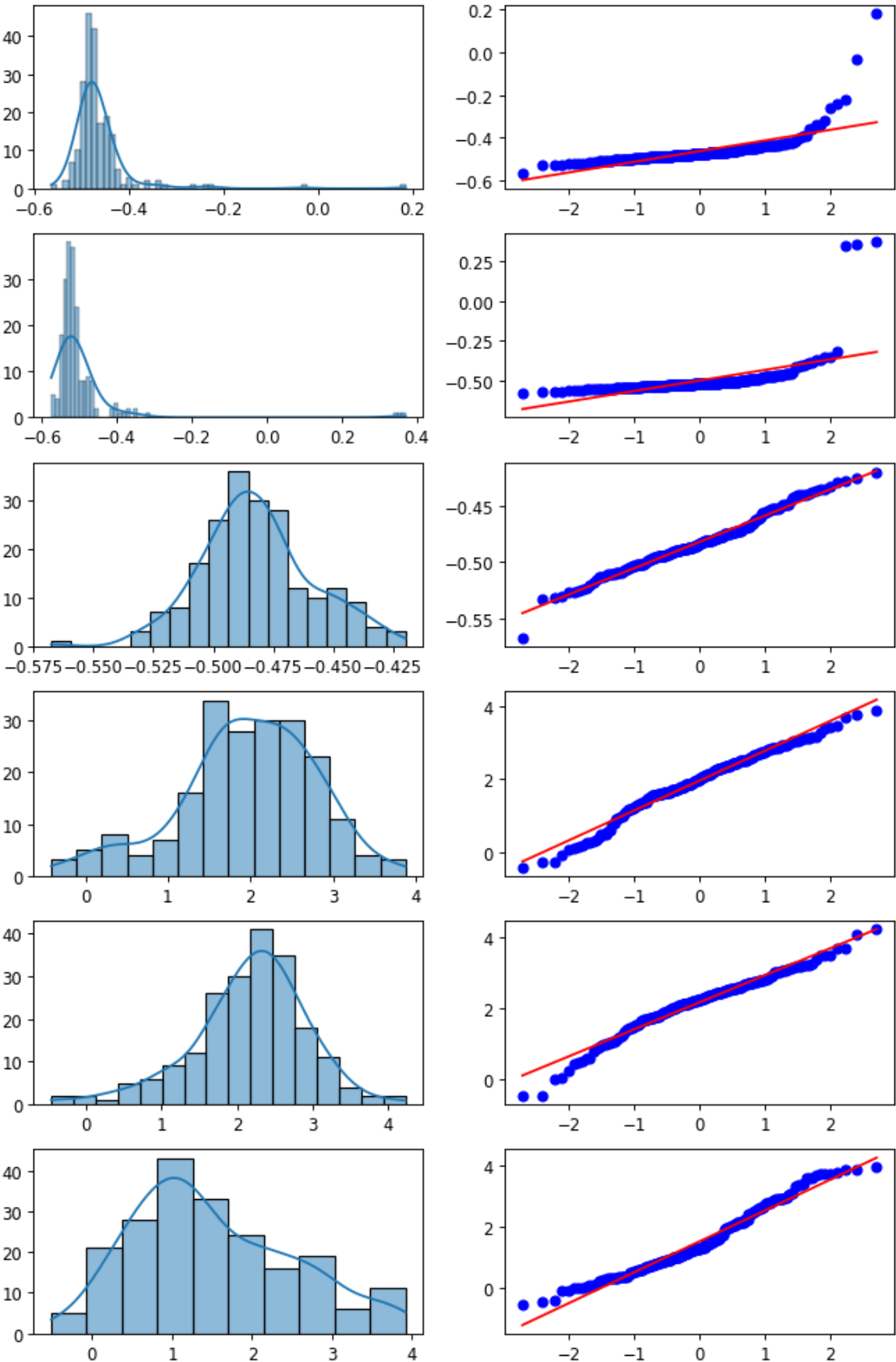


Figure 2. Histograms and Q-Q plots for the top six principal components of the class feature space of a randomly selected class prototype in Shrec-2017, with each row indicates a component.